16th International Conference on Greenhouse Gas Control Technologies, GHGT-16

23rd -27th October 2022, Lyon, France

Suitability and optimisation of analytical indoor shelter model used for infiltration of carbon dioxide for typical dwellings

B. Wetenhall[*a], J.M. Race[b], K. Adeflia[b], B. Aktas[b], H. Aghajani[a,c], C. Lyons[d], N. Reppas[a]

aSchool of Engineering, Newcastle University, Newcastle upon Tyne NE1 7RU, UK
bDepartment of Naval Architecture, Ocean and Marine Engineering, University of Strathclyde, Henry Dyer Building, Glasgow, G4 0LZ, UK
cHeraeus Conamic UK Ltd., Neptune Road, Wallsend, Tyne & Wear NE28 6DD UK
dPipeline Integrity Engineers Ltd., 262A Chillingham Road, Heaton, Newcastle-upon-Tyne, NE6 5LQ, UK

Abstract

Carbon Capture Utilisation and Storage (CCUS) schemes involve transporting large quantities of carbon dioxide (CO_2). A release of CO_2 from CCUS transportation infrastructure could cause severe consequences for the surrounding population if the risk is not appropriately managed. Following a release of CO_2, people in the surrounding environment could move away and seek shelter. The CO_2 plume could drift past buildings causing the concentration of CO_2 inside these buildings to build up. How much CO_2 accumulates inside the buildings is key to the safety of their occupants.

Previously an analytical infiltration model, based on wind and buoyancy driven ventilation, and a CFD infiltration model were created which can be used to predict the effect of CO_2 exposure on building occupants following a release from an onshore CO_2 pipeline [1]. These models can be used to determine the consequences of failure the dispersion behaviour of CO_2 and the infiltration rate of a plume of CO_2 into buildings and can form part of a Quantitative Risk Assessment (QRA) process for a CO_2 pipeline.

The models were validated against an experimental test of CO_2 infiltration into a small enclosure. Comparisons were made between the analytical model, CFD model and experimental data for the build-up of CO_2 in the enclosure and the changes in internal temperature.

This paper investigates the suitability of the analytical model for buildings geometries more closely resembling domestic abodes and against a wider range of conditions by comparing its results to those of the CFD model for a set of representative case studies. It also tunes the parameters used in the model.

Thirty test cases were created which explore the key parameters affecting the CO_2 ventilation rate: wind speed, the area and height of the openings, internal temperature and building height, width and length. The analytical model's predictions of the accumulation of CO_2 inside a building are shown to be extremely close to the CFD results for all cases except one, where it makes an over prediction of the level of CO_2. Furthermore, it is recommended that the analytical infiltration model is used with the tuned set of coefficients identified in this paper.

Keywords: CO_2 pipelines; CO_2 dispersion; Quantitative risk assessment; Consequence analysis; Shelter model; Model tuning

1. Introduction

Reducing anthropogenic carbon dioxide (CO_2) emissions is a key part of mitigating global climate change. Carbon Capture, Utilisation and Storage (CCUS) schemes are one accepted strategy of reducing CO_2 emissions from industrial and power generation installations. In CCUS schemes, CO_2 is captured at a large stationary emitter and transported

for either permanent storage in a geological formation or to be processed into a useful substance for commercial use. For the onshore transportation of CO_2, pipelines are generally regarded as the most economical mode of transport.

At standard conditions CO_2 is a colourless, odourless gas which is denser than air and undetectable by human senses. The current average concentration of CO_2 in air is over 400ppm [2]. However, in high concentrations CO_2 is an asphyxiant and can have toxic effects above 4% by volume [3]. Furthermore, due to its high density, CO_2 will displace air at ground level and, depending on environmental conditions, can accumulate in topographic dips and depressions such as valleys. CCUS schemes involve large quantities of CO_2 and a release from CCUS infrastructure, including pipelines, could cause severe consequences for the surrounding population if the risk is not appropriately managed.

To access the potential risks of onshore CO_2 pipeline transportation Quantitative Risk Assessment (QRA) procedures can be put in place to determine individual and societal risks. The procedure involves identifying the hazard scenarios then calculating the probability and consequences of failure. To determine the consequences of failure of CO_2 pipelines requires knowledge of the dispersion behaviour of CO_2 and the infiltration rate of a plume of CO_2 into buildings.

Following a pipeline rupture, the CO_2 will begin to depressurise to atmospheric pressure. This could involve a phase change to the gaseous and solid phases. The initial outflow is driven by the pressure difference between the surroundings and the internal pressure of the pipeline. The expanding CO_2 can cool to very low temperatures due to its high Joule-Thomson expansion coefficient and it will condense the water in the surrounding air to form a visible white plume. The plume gives an indication of the concentration of CO_2 to levels of 1% by volume [4] which is lower than levels that cause harmful effects. Once expanded to atmospheric pressure, the white plume of CO_2 will begin to disperse and drift depending on wind flow and other environmental conditions. The CO_2 plume could drift towards buildings causing the concentration of CO_2 inside these buildings to increase as CO_2 enters through windows, doors and adventitious openings. The amount of accumulation of CO_2 inside the buildings is key to the safety of their occupants.

In [1] Computational Fluid Dynamics (CFD) and analytical shelter models were created which can be used to predict the accumulation of CO_2 inside a building following a CO_2 pipeline release. The models can be used as part of a CO_2 pipeline QRA process to determine the level of exposure of CO_2 to the surrounding population. The models were validated against experimental data coming from a CO_2 infiltration test into a small, single storey enclosure. No impurities in the CO_2 stream assumed.

This paper tests the suitability of the analytical infiltration model developed in [1] for use with buildings geometries more closely resembling domestic abodes and against a wider range of conditions by comparing its results to those of the CFD model. The parameters within the analytical model are also tuned to capture the CFD results as closely as possible.

2. Previous infiltration models

The analytical model [1] works on the principle of natural ventilation, where flow is driven by wind and buoyancy effects caused by pressure differences between the interior and exterior of the building and by temperature differences within the building. The model extends [5] by combining both wind and buoyancy driven ventilation mechanisms in the manner of Etheridge and Sandberg [6,7].

Alongside the analytical model, a CFD CO_2 infiltration model was created using STAR-CCM+ [8] with the Reynolds Averaged Navier-Stokes (RANS) equations. The models use external temperature and CO_2 concentration as inputs and can predict the rate of CO_2 accumulation in an enclosure engulfed by a plume of CO_2. They were validated against a test of CO_2 infiltration into an enclosure, full details of the test are given in [1].

2.1. Analytical infiltration model

In the analytical model the concentration of CO_2 inside the enclosure is assumed to be uniform i.e. there is no variation with height or location. The model calculates the volumetric flow rate at a height z through an opening, $Q(z)$, using

$$Q(z) = C_d W(z) \sqrt{\frac{2|\Delta P|}{\rho}}$$ (1)

where C_d is a discharge coefficient, $W(z)$ is the width of the opening at a height z and ρ is fluid density. The pressure difference between inside and outside at a height z, $P(z)$, is found using

$$\Delta P(z) = \frac{1}{2} C_{sp} \rho_{ext} U_{wind}^2 - P' + gz$$ (2)

where C_{sp} is a surface pressure coefficient, ρ_{ext} is the pressure of the external fluid, U_wind is the incident wind speed, P^0 is a pressure that is determined by the location of the zero pressure level and g is gravitational acceleration.

The total flow of CO_2 into the enclosure, Q_{in}, and the total flow of CO_2 out of the enclosure, Q_{out}, are found using Simpson's rule:

$$\int_0^{z_0} Q_{in}$$ (3)

$$\int_{z_0}^h Q_{out}$$ (4)

respectively where z_0 is the neutral pressure level, the height where the internal and external pressures are equal, and h is the height of the building.

Densities are calculated using the ideal gas law and by assuming that the air and CO_2 are perfectly mixed. The change in internal concentration, C_{int}, in a time step dt then is

$$dC_{int} = \frac{Q_{in} - Q_{out}}{V_b} dt$$ (5)

where V_b is the volume of the enclosure.

The change in internal temperature is determined by assuming ideal gas behaviour, conservation of mass, perfect mixing inside the enclosure and that the specific heat capacities of CO_2 and air are roughly equal which leads to

$$\frac{dT_{int}}{dt} = \frac{1}{\rho_{int} V_b} \frac{d(\rho_{ext} Q_{in})}{dt} (T_{ext} - T_{int})$$ (6)

where T_{int} is the temperature inside the enclosure (assumed constant) and T_{ext} and ρ_{ext} are the temperature and density of the fluid entering the enclosure respectively.

The process is solved iteratively for P^0 with the condition of having steady state flow. At each time step the internal concentration and temperature is updated. Using this procedure, it is possible to calculate the change in internal CO_2 concentration over time.

To reproduce the experimental results the geometry of the test enclosure was used as input to the model, except that the size of the upwind opening was used for both openings. The discharge coefficient, pressure coefficient at the front of the building and pressure coefficient at the back of the building were set to 0.61, 0.7 and −0.25 respectively following [5].

2.2. CFD infiltration model

The CFD model was built in STAR-CCM+ and solves the equations for continuity of mass, momentum and energy as well as chemical species (in this case, oxygen, CO_2 and nitrogen). The humidity of the air was neglected and the air and CO_2 mixture was treated as a single phase fluid. The Reynolds Averaged Navier-Stokes equations were used with the standard turbulence model [9] and the Lag Elliptic Blending (EB) model [10] to incorporate the effect of buoyancy driven flows with low Reynolds number. Instantaneous values of κ and ϵ for the chosen model were obtained from the transport equation.

A Computer Aided Design (CAD) model was used to replicate the building used in the experiment which was imported into Star-CCM+. A polyhedral mesh was chosen with 45,000 cells and a prism layer mesher was used in the

near-wall regions. The walls, celling and floor were modelled as smooth solid boundaries and the no-slip condition was applied. It was further assumed that there was no heat flux between the walls and the fluid. Any initial turbulence in the building was neglected. The pressure at the outlet was assumed to be atmospheric pressure, any existing initial turbulence was ignored in the model, the flow was incompressible. The ideal gas law was used to calculate density. The setup used a maximum Courant-Freidrichs-Lewy (CFL) Number of 10 and a mean CFL Number of 5 over the whole domain.

2.3. Previous comparison with experimental data

Comparisons were made between the analytical model, CFD model and experimental data for the build-up of CO_2 in the enclosure and the changes in internal temperature.

Experimental measurements of CO_2 accumulation within the enclosure were taken as a cloud of drifting CO_2 passed the enclosure following a scaled pipeline rupture experiment that was conducted as part of the National Grid COOLTRANS research programme [11]. The wind was incident on the front face of the enclosure at an angle of approximately 20 degrees from the normal with an average speed of 1.17 m/s. The enclosure was 3.5 m by 3.5 m and 3 m high with metal sheet sides, a roof and no internal partitions. It was sealed apart from two openings: one 1.04 m high by 0.24 m wide and positioned upwind and the other 1.04 m high by 0.22 m wide and positioned downwind. The height from the floor to the bottom of the windows was 1.3 m.

The analytical and CFD models used the experimental average wind speed and direction. The temperature and CO_2 concentration at the inlet were used as inputs to the models with a frequency of 1 second. The models then predicted the accumulation of CO_2 in the enclosure over time. The models both produced very similar results and tended to slightly over predict the concentration of CO_2 inside the enclosure.

The ventilation rate into the enclosure was much higher than would be expected for a typical domestic house so that a measurable quantity of CO_2 built up inside the enclosure during the timescale of the experiment. This paper tests the analytical model's predictions against those of the CFD model for a series of realistic case studies.

3. Testing the Analytical Model in Further Scenarios

To test the analytical model at building geometries more closely resembling domestic abodes and against a wider range of conditions, thirty test cases were created which explore the key parameters affecting the CO_2 ventilation rate. These are wind speed, the area and height of the openings, internal temperature and building height, width and length. The ranges of the variables are shown in Table 1 and a schematic of the building in Figure 1.

Table 1. Range of case study parameters

	Minimum Value	Maximum Value
Wind speed (m/s)	2	30
Area of openings (% of total area of face)	0.02	2
Internal temperature (℃)	5	20
Vertical distance to bottom of openings (% of total height of wall)	30	50
Room height (m)	2	6
Room length (m)	-4	12
Room width (m)	4	12

Figure 1: Schematic of the building
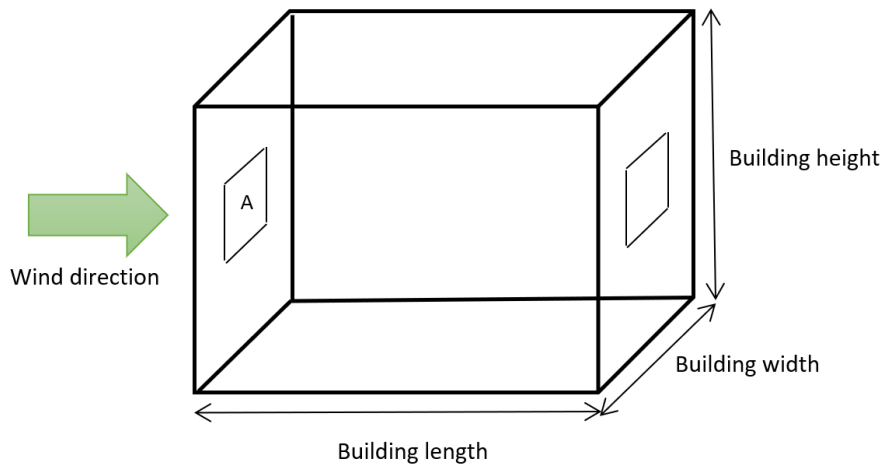
The minimum width and length were chosen based on [12] which state that a single bedroom should be at least 2.15m wide (rounded down to 2m). The minimum height was based on UK building regulations which state that the minimum floor to ceiling height should be a minimum of 2.3m (rounded down to 2m) for at least 75% of the Gross Internal Area [13]. The minimum temperature was chosen to be 5°C based on the boiler frost temperature of a typical boiler [14]. There is no maximum temperature for buildings in UK law and therefore a maximum temperature of 20°C was chosen, based on the average maximum temperature for July across the UK [15]. The wind range was selected based on the Beaufort wind force scale and ranged from a light breeze to a violent storm. The maximum sizes, the range of opening areas and the heights of the beginning of openings were estimated based on typical buildings around the UK.

From the ranges of the variables, a set of thirty test cases was generated using a maximum Latin hypercube design to ensure an even spread in the parameter space. The cases are shown in Table 2.

The analytical model predicts the changes to internal concentration and temperature over time. To compare the results of the analytical and CFD models over the thirty cases three key prediction metrics were identified:

- The peak concentration reached in a case
- The integral of the concentration over the length of time of the release[*] (the area under the time/concentration plot)
- The time to reach the short term exposure limit (STEL) of CO_2

The short term exposure limit was set to 1.5 % (15 minute reference period) according to [16]. The integral of the concentration over the length of time of the release is the most important parameter as limiting the exposure to CO_2 over time is the primary driver for a risk analysis. The peak concentration prediction is also required as high concentrations of CO_2 are an asphyxiation hazard. The metrics are illustrated in Figure 2.

---

[*]For the results of this paper an order 6 polynomial regression was used to generate the curve used for the integral. Regressions from the CFD results have R^2 values between 0.963 and 1.000 and regressions from the analytical model results have R^2 values between 0.968 and 1.000.

Table 2: Parameter values for each test case

Case	Building Height (m)	Building Width (m)	Building Length (m)	Wind Speed (m/s)	Window Area (% of face)	Initial Internal Temperature	Height of Bottom (% of height)
1	3.38	8.14	7.86	7.79	0.57	11.21	43.79
2	2.41	5.10	10.34	11.66	1.45	19.48	38.97
3	4.62	4.83	8.97	3.93	1.80	7.59	43.10
4	5.86	11.17	5.38	15.52	0.36	16.90	44.48
5	5.72	4.55	10.90	26.14	0.77	12.76	34.83
6	5.45	9.79	4.00	16.48	0.02	5.52	45.86
7	2.97	9.52	5.93	25.17	2.00	9.66	47.24
8	2.00	4.00	6.48	12.62	1.86	12.24	45.17
9	3.10	7.03	4.83	14.55	1.39	7.07	38.28
10	4.07	12.00	4.55	29.03	0.29	8.62	35.52
11	2.28	7.59	9.79	6.83	0.50	10.69	30.00
12	5.31	5.93	5.10	2.97	0.09	8.10	41.72
13	5.59	6.21	9.24	10.69	0.63	16.38	46.55
14	2.14	10.62	7.59	18.41	1.11	15.86	50.00
15	4.76	10.34	7.03	28.07	1.59	17.93	42.41
16	5.17	8.69	8.14	5.86	0.22	18.45	33.45
17	3.66	10.07	10.07	24.21	0.91	10.17	40.34
18	5.03	11.45	8.69	8.76	0.84	6.03	36.90
19	4.21	5.66	7.31	22.28	1.25	13.28	47.93
20	6.00	11.72	11.45	13.59	0.98	15.34	49.31
21	3.52	5.38	4.28	30.00	0.43	13.79	36.21
22	3.24	7.86	11.72	27.10	1.04	20.00	34.14
23	4.90	7.31	8.41	17.45	1.66	14.83	32.07
24	4.34	4.28	9.52	20.34	1.18	5.00	41.03
25	4.48	6.76	6.21	21.31	0.16	6.55	32.76
26	3.93	8.41	12.00	9.72	1.73	17.41	48.62
27	2.83	6.48	10.62	23.24	1.52	9.14	30.69
28	3.79	10.90	11.17	4.90	1.32	11.72	31.38
29	2.69	8.97	5.66	19.38	0.70	18.97	37.59
30	2.55	9.24	6.76	2.00	1.93	14.31	39.66

Figure 2: Illustration of the key prediction metrics used
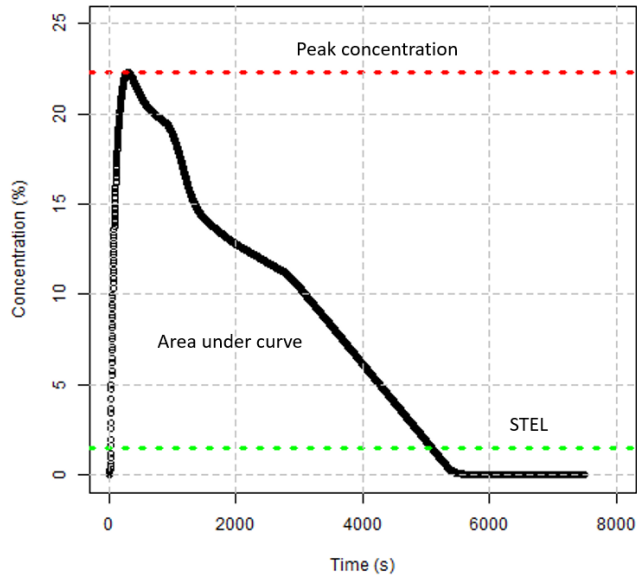
3.1. Comparing the analytical and CFD models over the further cases

To compare the results of the analytical and CFD infiltration models over the further cases the same external temperature and concentrations were used as inputs for each case in both models. The profiles were generated using an in-house flat terrain dispersion model created by DNV-GL developed from the results of COOLTRANS experiments [17, 18] and are shown in Figures 3 and 4. A double ended guillotine break type rupture is assumed to occur at the mid-point of a 96 km long dense phase CO_2 pipeline and valve closure is set to 15 minutes after the start of the release. The temperature of the CO_2 in the pipeline is assumed to be 30∘C and the wind speed 5 m/s. The CO_2 cloud dispersion was modelled for two hours following the rupture. Details of the pipeline parameters which remain constant between each simulation are provided in Table 3. The wind was assumed to be blowing directly onto the face of the enclosure and the building is located 100m from the release.

Table 3: Dispersion Model Inputs

Input	Value
Length	96 km
Outside Diameter	610 mm
Wall Thickness	19.4 mm
Internal Pressure	150 barg
Material	Carbon Steel

Figure 3: Concentration profile used as an input to the models for the 30 cases [18]

External Concentration of CO$_2$
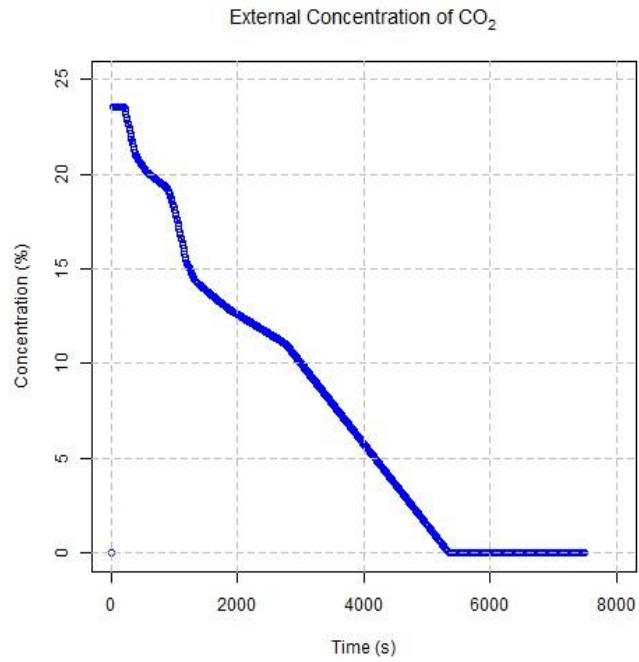
Figure 4: Temperature profile used as an input to the models for the 30 cases [18]

External Temperature of CO$_2$
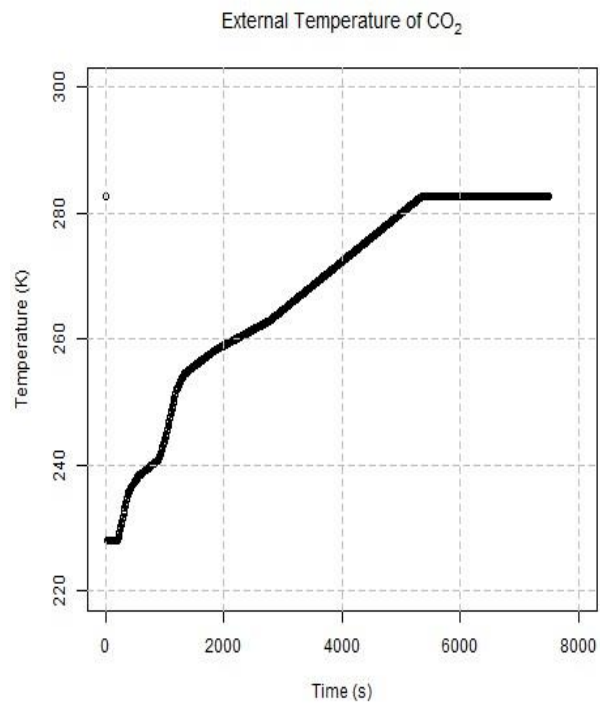
Using the concentration and temperature inputs from above, the models from Section 2 were then run for each of the thirty cases to generate the change in internal CO_2 concentration over time. To generate an average concentration from the CFD model (needed for comparison to the analytical model), CO_2 measurements were averaged from sensors placed inside the building which are 5cm apart in vertical planes that are in line with the windows and cover the cross section of the building, as in Figure 5. The mesh of an example case is shown in Figure 6. A comparison between the models for each case is shown in Appendix A. The identified metrics for each case were also compared and these are shown in Table 4 where the ratios are the analytical model results/CFD model results.

Figure 5: Example of the placement of CO2 sensors in the CFD model
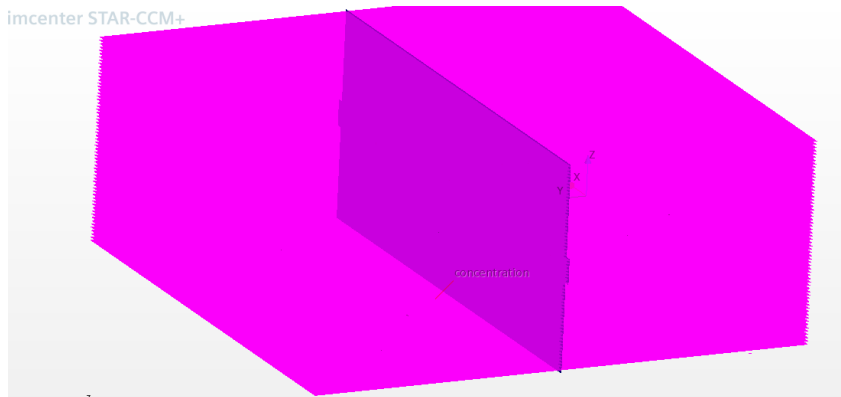
Figure 6: Example of the mesh of the CFD model for one of the cases. The openings are shown in yellow.

Looking across all the cases, all of the analytical integrals are within 3% of the CFD integrals except in three cases. Case 16 shows the largest difference between the analytical and CFD integrals where the analytical integral is 21 % higher than the CFD integral. The other cases in excess of a 3 % difference are Case 10 and Case 12, where the analytical integral are 6 % and 16 % lower than the CFD integral respectively.

The peak concentration predictions show greater variance between the models. Here, a total of 10 cases

show a deviation of 10 % or more between the predictions of the models. The analytical model tends to under predict the peak concentration compared to the CFD model except in Cases 15, 16, 21 and 22. Cases 6, 16 and 30 show the largest deviations between the models (21 %, 19 % and 20 % respectively).

Apart from Case 23, the analytical model predicts a shorter time to reach the short term exposure limit of CO_2. The values differ more for Cases 1, 3, 6, 12, 13, 16 and 30 which show a factor of two difference between the predictions of the model. However, both models predict that the short term exposure limit is reached within 5 minutes and the only cases that differ by more than 100 s are Cases 6 and 12. The only case that the CFD model predicts a longer time to reach the short term exposure limit is Case 23, where it predicts that the limit is reached 2 seconds after the prediction by the analytical model.

Overall, the analytical model is able to reproduce the results of the CFD model to a reasonable degree. The models tend to disagree for small window areas and low wind speeds which is considered to be a result of a low rate of air change between the building and its surroundings. When pressures generated by wind are negligible then ventilation flow rate calculations have the highest level of uncertainty [7].

4. Optimising the Analytical Model in Further Scenarios

There are three coefficients in the analytical model: two pressure coefficients and a discharge coefficient as seen in Equations 1 and 2. In ventilation models, pressure coefficients are a dimensionless parameter used to express the pressure differences between the inside and outside of a building. They are positive when the wind is causing a flow into the enclosure and negative when the wind is causing a flow out of the enclosure. The pressure difference at the front and back of a building will differ so pressure coefficients are needed for the front (C_{pFront}) and back (C_{pBack}) of a building. For this study the wind is assumed incident on the front face of the building but either coefficient can be still negative or positive depending on the angle of the wind direction. The discharge coefficient (C_d) is a dimensionless parameter measuring the resistance to flow an opening has. It is defined as the ratio of the actual discharge to the theoretical ideal discharge.

For air at standard pressure and temperature, typical values of C_{sp} in the UK vary between 0 and 1.2 [19] and the values will change with wind speed and direction. C_{sp} can usually determined as a function of building geometry and surrounding topography using experimental or numerical testing, for example wind tunnel tests and CFD modelling. The discharge coefficient has a constant value for each type of opening the building has and changes depending on the size and shape of the opening. For high flow rates there is reduced dependence on C_d [7].

As far as the authors are aware, no data exists for CO_2 pressure coefficients so this paper uses the pressure and discharge coefficients as tuning parameters in the analytical model to find the best combination for predicting the CFD model results across all the thirty case studies. The primary goal is to match the integral of the concentration over the time of the simulation (performed in the same way as in Section 3) as this is the most important for a risk assessment. However, the peak concentration and time to reach the short-term exposure limit are also compared. The best set of coefficients is defined as the one for which there is the least total deviation from the CFD integrals.

4.1. Finding the Optimum set of Coefficients

To tune the coefficients of the analytical model, the pressure and discharge coefficients were independently varied from their original values (both decreased and increased). The values were varied until the areas under the regressions of the analytical model began to diverge from the CFD model regression areas. The range of the coefficients is shown in Table 5.

Table 4: Metrics generated from the analytical and CFD results

Case	Integral Ratio	Peak Concentration Ratio	Time to Limit Ratio
1	0.98	0.84	2.31
2	1.00	0.91	1.58
3	1.02	0.97	2.27
4	0.99	0.99	1.33
5	1.00	0.98	1.15
6	0.90	0.79	2.13
7	1.00	1.00	1.25
8	1.00	0.90	1.88
9	0.99	1.00	1.18
10	0.99	1.00	1.20
11	1.00	0.83	1.82
12	0.84	0.84	2.55
13	0.99	0.84	2.00
14	1.00	0.89	1.58
15	1.00	1.03	1.05
16	1.21	1.19	2.16
17	1.00	0.99	1.15
18	0.99	0.99	1.43
19	1.00	0.93	1.58
20	1.00	0.90	1.67
21	1.00	0.99	1.00
22	1.00	1.01	1.15
23	1.00	1.01	0.91
24	1.00	0.98	1.36
25	0.99	0.91	1.39
26	1.00	0.87	1.60
27	1.00	0.99	1.05
28	1.01	0.93	1.79
29	1.00	0.96	1.50
30	1.03	0.80	2.80

   Simulations of the analytical model were then performed using the full set of combinations of coefficients covering the range from their minimum to their maximum values in increments of 0.1. This gives a total of 4800 unique combinations of coefficients. The analytical model was run for each set of coefficients for each of the thirty case studies and the integral of each set of concentration/time results was performed. These were then compared to corresponding results generated by the CFD model. The best set of coefficients was deemed as the one having the minimum total divergence from the CFD integrals when considering all thirty cases. The results of the peak concentrations and the time to reach the short-term exposure limit were also compared to those of the CFD model.

Table 5: Range of pressure and discharge coefficients

	min	max
C_d	0.1	1
C_{pFront}	0.2	2.5
C_{pBack}	-1.8	0.1

   Comparing the results of the regression integrals, many coefficient combinations matched the CFD data well: over 4000 combinations had a total deviation of less than 5%. There were 17 coefficient combinations that showed almost indistinguishably the best performance. All had $C_d = 0.7$ and $C_{pFront} - C_{pBack} = 1.7$ with all having the same total error of 1.25% for the regression integrals. Plots of concentration against time generated for each case from the analytical model with the best set of coefficients and the CFD model are shown in Appendix B and a comparison of the metrics to the CFD results is shown in Table 6 (the case with $C_d = 0.7$, $C_{pFront} = 1.5$ and $C_{pBack} = -0.2$ is chosen for illustration and the ratios are the analytical model results/CFD model results).

   Each of the 17 best combinations predicted the same peak concentrations and time to reach short-term exposure limit, which when comparing with the CFD case have R^2 values of 0.93 and 0.89 respectively. For reference, the base case (with the coefficients set as in [1]), regression integrals have a total error of 2.3% and the peak concentrations and time to reach short term exposure limit have R^2 values of 0.88 and 0.85 respectively. The worst combination ($C_d = 0.1$, $C_{pFront} = 0.2$, and $C_{pBack} = 0.1$) had a total error of 28% for the integrals.

   For the best combination of coefficients, all the analytical integrals were within 2% of the CFD integrals except for Case 16 where the analytical integral is 20% higher. This is an improvement on the base case which has an analytical integration which is 21% higher than the corresponding CFD integral for Case 16 but also has large errors for Case 12 (16% under prediction) and Case 6 (10% under prediction) which the best combinations do not.

   Overall, looking across the thirty case studies, the base case is able to predict the results of the CFD model well but can be improved upon using the best coefficient combination. For Case 16, the analytical model finds it difficult to predict the results of the CFD model. This case has a medium volume enclosure and low wind speed and the analytical model gives conservative results.

Table 6: Metrics generated from the analytical best case and CFD results

Case	Integral Ratio	Peak Concentration Ratio	Time to Reach Limit Ratio
1	0.98	0.93	1.54
2	1.00	0.97	1.58
3	1.02	1.05	1.82
4	0.98	1.04	1.00
5	1.00	1.04	1.15
6	1.00	0.95	1.49
7	1.00	1.02	1.25
8	1.00	0.95	1.88
9	0.99	1.02	1.18
10	0.99	1.06	1.20
11	1.00	0.94	1.52
12	1.00	1.07	2.17
13	0.99	0.93	1.33
14	1.00	0.94	1.58
15	1.00	1.06	1.05
16	1.24	1.39	1.57
17	1.00	1.05	1.15
18	0.98	1.04	1.07
19	1.00	0.99	1.05
20	0.99	0.96	1.33
21	1.00	1.03	1.00
22	1.00	1.05	0.77
23	1.00	1.04	0.91
24	1.00	1.03	0.91
25	0.99	0.98	1.11
26	1.00	0.92	1.20
27	1.00	1.02	1.05
28	1.01	0.99	1.43
29	0.99	1.00	1.00
30	1.02	0.92	2.00

5. Conclusions

In [1], analytical and CFD CO_2 infiltration models were created which can predict the build up of CO_2 inside an enclosure following a release of CO_2. Results from the models were compared against an experimental study of CO_2 infiltration into a small enclosure. The motivation for the models was for use in a QRA for dense phase CO_2 pipelines. This paper tests the accuracy of the analytical model for use in wider more realistic scenarios by comparing its results with those of the CFD model. Thirty potential scenarios were created and the results of the models compared using three metrics: peak concentration value, the time to reach the short-term exposure limit and the area under the concentration-time plot using a 6 order regression. The analytical model shows good predictions for the majority of cases however its results tend to diverge for small window areas and low wind speeds where there will be a low rate of air change in the building.

To attempt to improve the predictions of the analytical model, tuning of its three parameters was undertaken by comparing results generated with different combinations of coefficient to the CFD results across the thirty case studies. A set of 17 combinations of coefficients (all with $C_d = 0.7$ and $C_{pFront} - C_{pBack} = 1.7$) were found that improve the performance of the analytical model matching the CFD results. All the predictions of the best sets are extremely close to the CFD predictions apart from in Case 16 where the analytical model over predicts the concentration of CO_2.

The set of pressure and discharge coefficients could be determined from wind testing under a variety of wind directions and speeds with different building/opening geometries. Until that is done, it is recommended that the analytical infiltration model is used with the best set of coefficients identified in this paper.

Acknowledgements

Appendix A. Comparing the analytical and CFD model results over the 30 cases
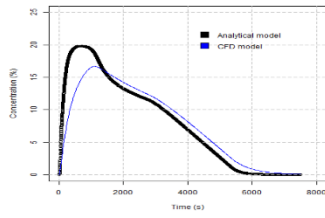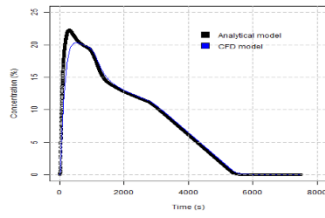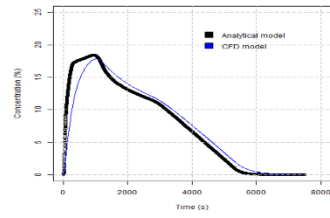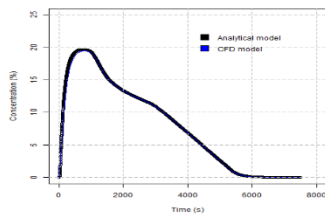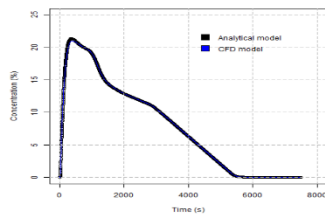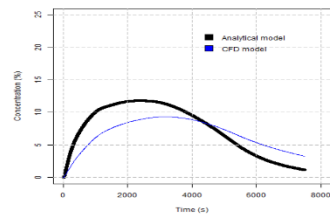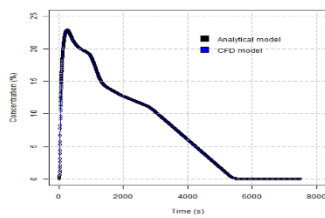
(a) Case 1

(b) Case 2

(c) Case 3

(d) Case 4

(e) Case 5

(f) Case 6
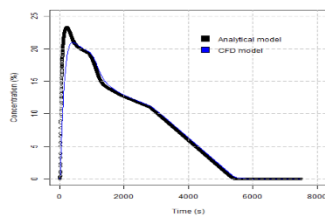
(g) Case 7
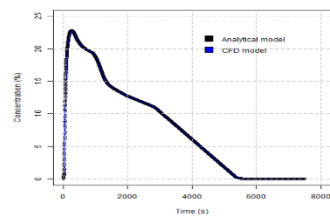
(h) Case 8
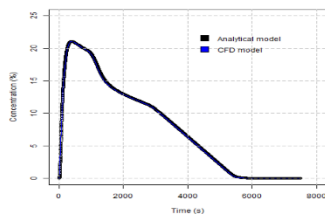
(i) Case 9
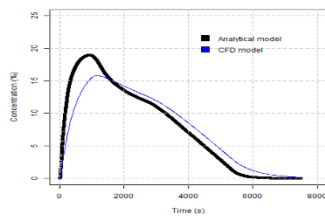
(j) Case 10
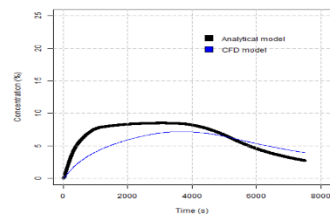
(k) Case 11
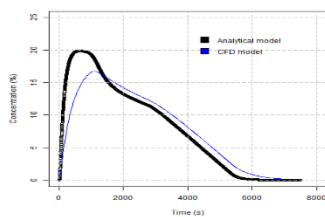
(l) Case 12
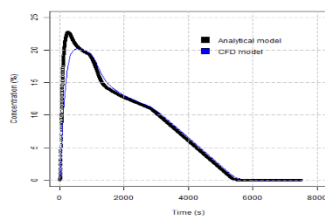
(m) Case 13
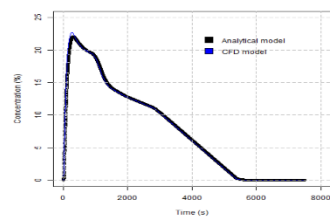
(n) Case 14
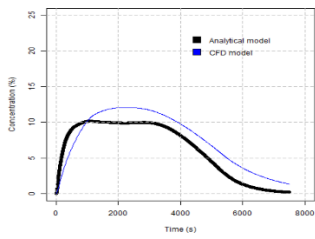
(o) Case 15
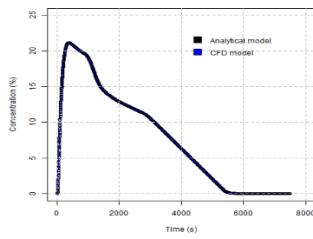
(a) Case 16
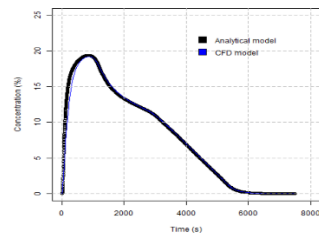
(b) Case 17
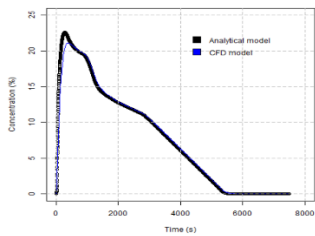
(c) Case 18
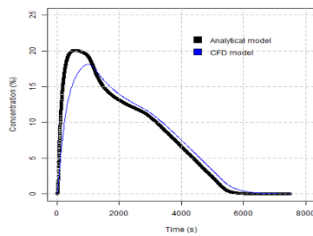
(d) Case 19
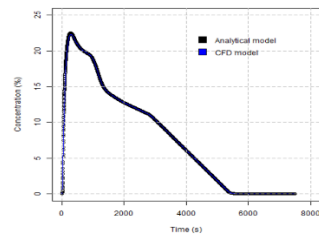
(e) Case 20
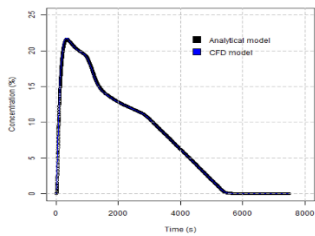
(f) Case 21
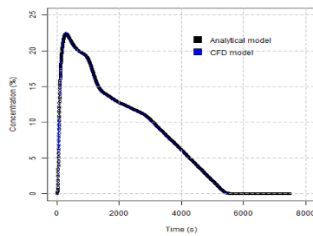
(g) Case 22
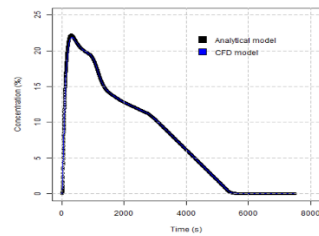
(h) Case 23
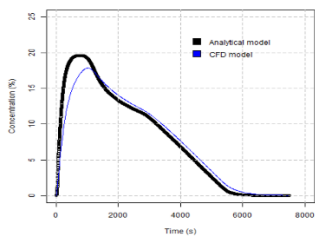
(i) Case 24
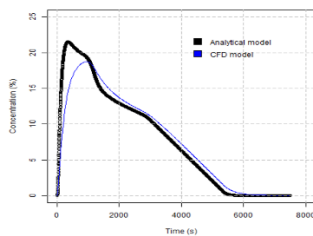
(j) Case 25
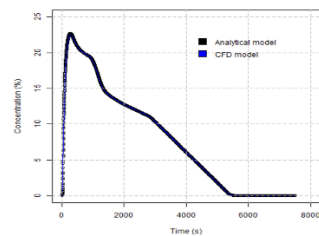
(k) Case 26
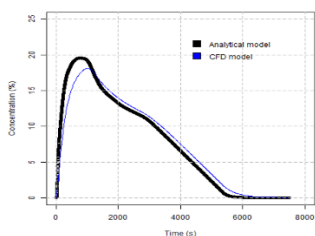
(l) Case 27
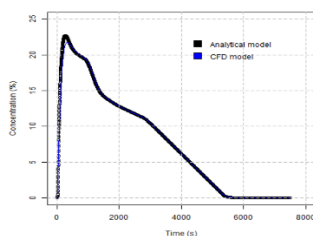
(m) Case 28
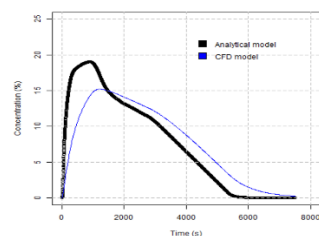
(n) Case 29

(o) Case 30

Appendix B. Comparing the analytical best case and CFD model results over the 30 cases
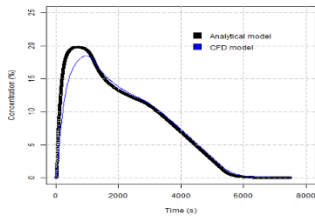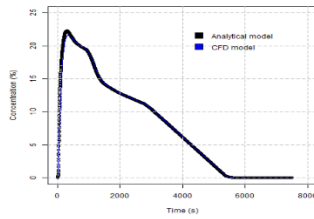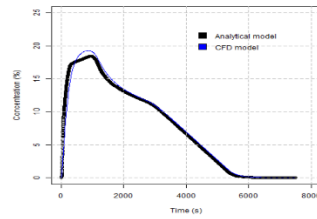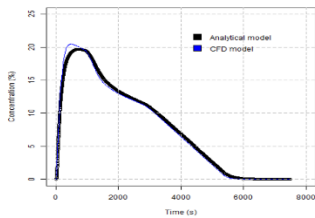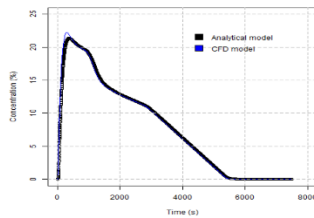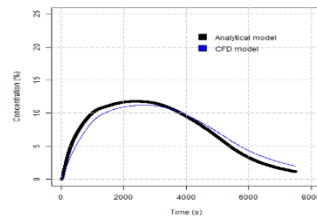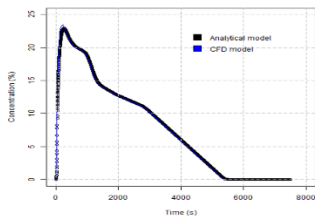
(a) Case 1

(b) Case 2

(c) Case 3

(d) Case 4

(e) Case 5

(f) Case 6
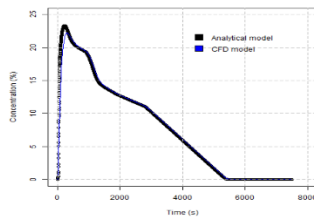
(g) Case 7
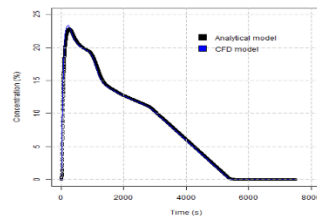
(h) Case 8
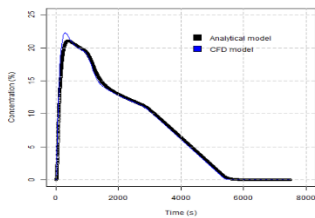
(i) Case 9
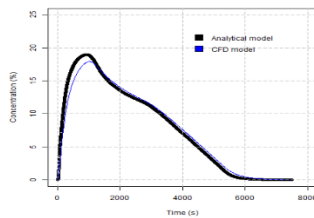
(j) Case 10
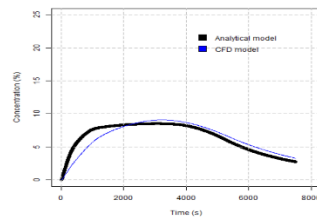
(k) Case 11
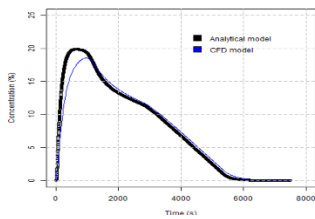
(l) Case 12
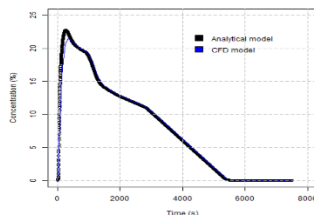
(m) Case 13
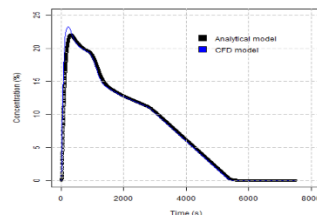
(n) Case 14

(o) Case 15

(a) Case 16
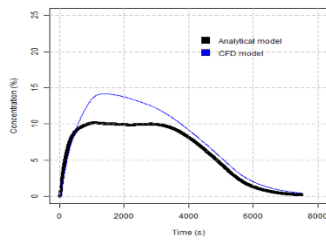
(b) Case 17
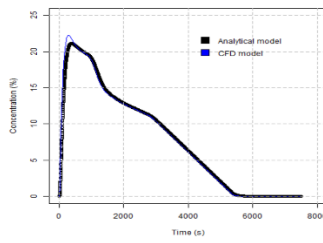
(c) Case 18
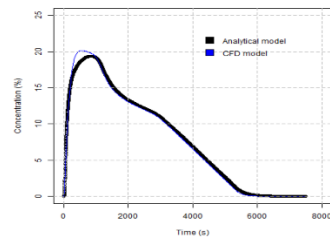
(d) Case 19
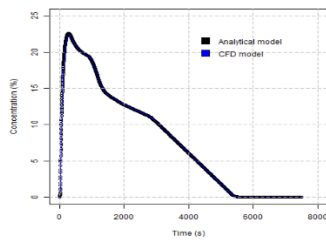
(e) Case 20
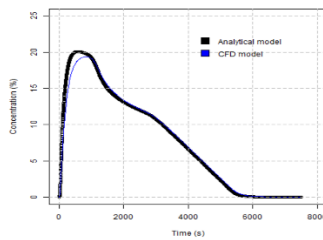
(f) Case 21
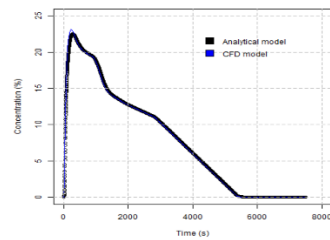
(g) Case 22
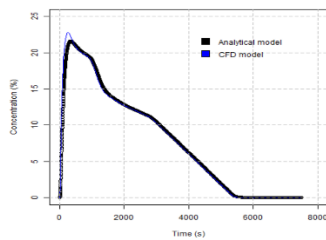
(h) Case 23
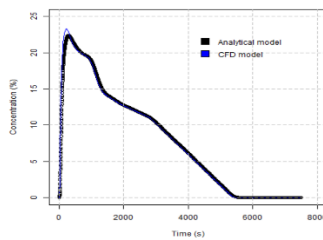
(i) Case 24
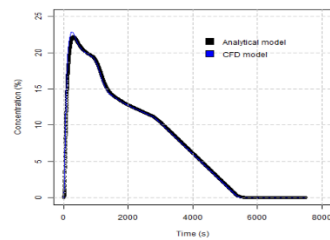
(j) Case 25
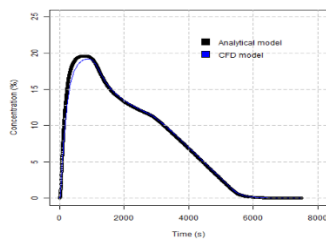
(k) Case 26
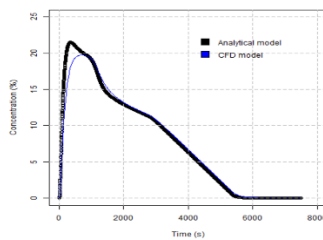
(l) Case 27
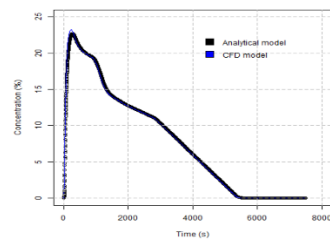
(m) Case 28
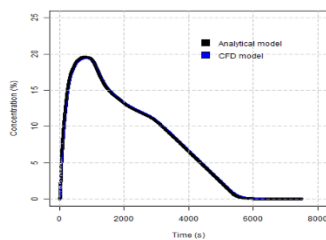
(n) Case 29
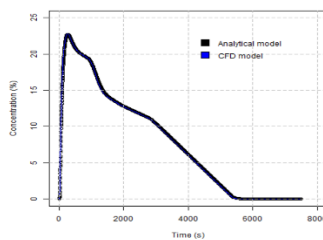
(o) Case 30
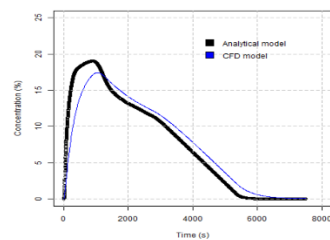
References

[1] Lyons, C.J.; Race, J.M.; Adefila, K.; Wetenhall, B.; Aghajani, H.; Aktas, B.; Hopkins, H.F.; Cleaver, P.; Barnett, J. Analytical and computational indoor shelter models for infiltration of carbon dioxide into buildings: Comparison with experimental data. Int. J. Greenh. Gas. Con. 2020, 92, 102849.

[2] Team EW. Earth System Research Laboaratories, Global Monitoring DivisionGlobal Greenhouse Gas Reference Network. Trends in Atmospheric Carbon Dioxide. 2022.

[3] Ikeda N, Takahashi H, Umetsu K, Suzuki T. The course of respiration and circulation in death by carbon dioxide poisoning. Forensic Sci Int. 1989;41(1):9399. doi: 10.1016/0379-0738(89)90240-5

[4] Wen, J., Heidari, A., Xu, B., Jie, H., 2013. Dispersion of carbon dioxide from vertical vent and horizontal releases A numerical study, May 2013.

Proceedings of the Institution of Mechanical Engineers Part E Journal of Process Mechanical Engineering 1989-1996 (vols 227(2):125-139

[5] BS5925, BS5925, 1991. Code of Practice for Ventilation Principles and Designing for Natural Ventilation. British Standards Institute, London, pp. 1991.

[6] Etheridge, D.W., Sandberg, M., 1984. A simple parametric study of ventilation. Build. Environ. 19, 16373.

[7] Etheridge, D.W., Sandberg, M., 1996. Building Ventilation: Theory and Measurement. John Wiley and Sons, New York.

[8] S.P. Software, 2016. STAR-CCM+ in.

[9] Launder, B.E., Sharma, B.I., 1974. Application of the energy-dissipation model of turbulence to the calculation of flow near a spinning disc. Lett. Heat Mass Transf. 1, 131137.

[10] Revell, A.J., Benhamadouche, S., Craft, T., Laurence, D., 2006. A stress strain lag Eddy viscosity model for unsteady mean flow. Int. J. Heat Fluid Flow 27, 821830.

[11] Allason, D., Armstrong, K., Barnett, J., Cleaver, P., Halford, A., 2012. Experimental studies of the behaviour of pressurised releases of carbon dioxide. 23rd Institution of Chemical Engineers Symposium on Hazards 142152.

[12] Department for Communities and Local Government, Technical housing standards a nationally described space standard, March 2015

[13] The Building Regulations 2010, Protection from falling, collision and impact, Document K.

[14] Ideal, User Guide Ideal Instinct 24 30 35

[15] Met Office, Mean daily maximum temperature - August average: 19812010

[16] HSE, EH40/2005 Workplace exposure limits, 2018.

[17] Barnett, J. and Cooper, R, The COOLTRANS Research Programme: Learning for the Design of CO2 Pipelines, Proceedings of the 2014 10th International Pipeline Conference IPC2014 September 29 - October 3, 2014, Calgary, Alberta, Canada.

[18] C.J. Lyons, J.M. Race, H.F. Hopkins, P. Cleaver, Prediction of the Consequences of a CO2 Pipeline Release on Building Occupants, Symposium Series no 160 Hazards 25, Edinburgh International Conference Centre, Edinburgh, UK on 13-15 May 2015.

[19] Wiren, B.G. Effects of surrounding buildings on wind pressure distributions and ventilation losses for single-family houses, Part 2: Two storey terrace houses. National Swedish Institute for Building Research, Research Report TN2, Gävle , Sweden, 1985.